Influence of Cold Working on the Mechanical Field around Creep Crack Tip of Stress Corrosion Cracking

Cui Yinghao[1], Zhao Lingyan[2, *] and Wang Weibing[1]

[1] School of Mechanical Engineering, Xi'an University of Science and Technology, Xi'an 710054, China
[2] School of Science, Xi'an University of Science and Technology, Xi'an 710054, China

*gloomy2@foxmail.com

Abstract. To understand the effect of cold working on the mechanical properties of stress corrosion cracking in 304 stainless steel, the influence of different cold working on the stress strain field near the crack front of 304SS was analyzed using ABAQUS. Results show that Mises stress will increase with increasing of the CW before creep. As the creep process is going on, the effect of cold working on the Mises stress around crack front will become weaker; Cold working will cause the decrease of the low-plasticity strain region at the crack front, but has little effect on the high plastic strain; Cold working will also cause the crack tip creep strain increase to a certain extent, indicating that the cold working will accelerate stress corrosion cracking to some extent.

1. Introduction

Stress corrosion cracking(SCC) is a failure mechanism that is caused by environment, susceptible material and tensile stress of nuclear power structural materials under high temperature and high pressure water environments [1]. During the manufacturing and assembly process under the nuclear power equipment, a certain degree of cold working will occur [2]. The amount of cold working will affect the stress corrosion rate and the crack tip mechanical state of the material in the nuclear environment. SCC caused by crack tip creep in high temperature water environment is one of the important factors lead to the failure of structures [3]. Therefore, it is very important to obtain accurate creep crack propagation rate for quantitative prediction nuclear structure life [4]. Many research shows that cold working has great effect on the creep mechanical field around crack tip [5-6].

Finite element model is established under different cold working using compact tension specimen using 304 stainless steel. The mechanical properties of crack tip region are studied.

2. Finite element modelling

2.1. Specimen model

The finite element analysis of the 1T-CT specimen was performed using the above material properties. The geometrical dimensions and the experimental procedure of the specimen confirmed to the ASTM399 standard [7], as shown in Figure 1.

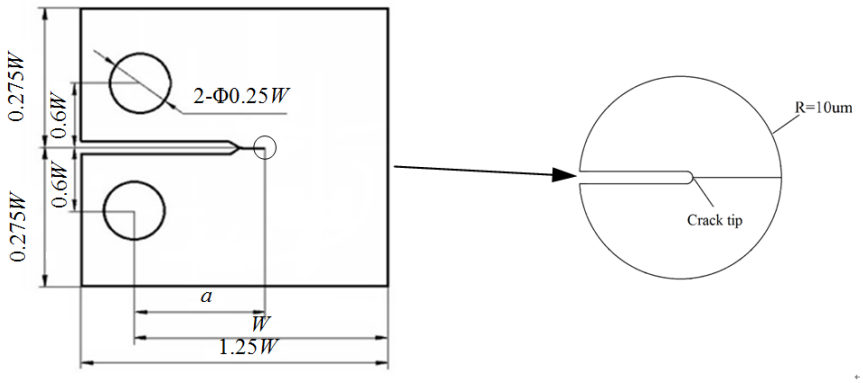

Figure 1. Geometry and dimensions of 1T-CT model

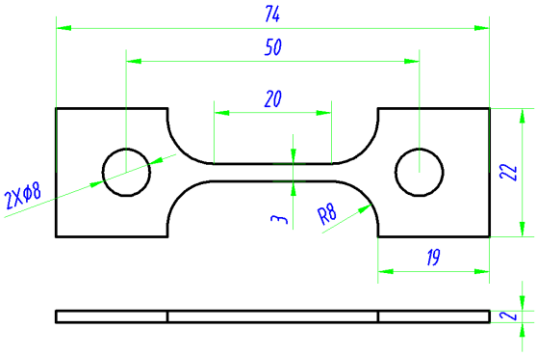

Figure 2. Plate tensile specimen of 304SS

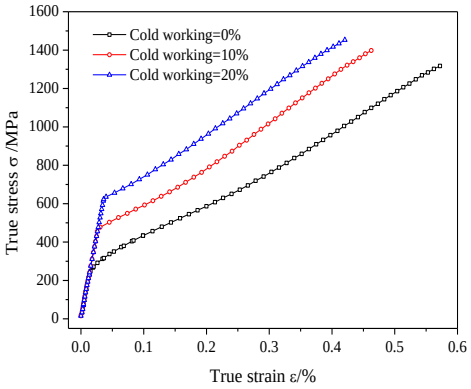

Figure 3. True stress-strain curves under different CW

2.2. Material model

The plate tensile specimen used in this study is 304 stainless steel and its geometry and dimensions are shown in Figure 2. Its chemical chemical composition includes C-0.043%, Si-0.4%, Mn-1.18%, P-0.033%, S-0.002%, Ni-8.04%, Cr-18.115%, N -0.046% etc. Tensile experiment was carried out in fatigue stretcher machine under different cold working rates, engineering stress and strain curve was derived and converted to true stress-strain curves. The material true mechanical curves was shown in Figure 3 under the amount of cold working is 0%, 10% and 20%, respectively.

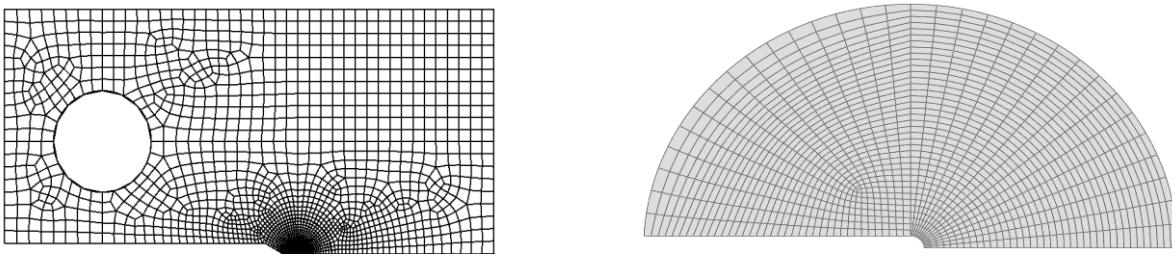

(a) Global mesh model (b) Mesh around the crack tip

Figure 4. Finite element mesh model of half model of 1T-CT

The creep rate is calculated using the power law model [8-9] in the FEM calculation:

$$\dot{\varepsilon}_{cr} = A\sigma^n t^m \quad (1)$$

Where $\dot{\varepsilon}_{cr}$ is the creep strain rate. σ is the applied stress; A is the power law multiplier, the value is 1.24×10^{-23}, n is the creep exponent, and the value is 7.5.

To eliminate the stress singularity generated by the crack tip [10], the crack tip radius was taken as 0.5μm in the finite element simulation. Because of the symmetry of the sample structure and load, 1/2 model was established in my study. The CPE8R was adopted in mesh type, as shown in Figure 4a. To obtain more detailed and accurate crack tip stress and strain, the mesh around crack tip was refined and its number was 15027, as shown in Figure 4b.

2.3. Loading and boundary conditions

Due to symmetry of CT specimen, only the half specimen was modelled. Boundary condition is applied to the symmetry plane of the model. Loading is applied to the load hole by using the multiple point constraints facility in ABAQUS, which joins the hole centre to the nodes of the whole surface. The concentrated force is applied on the reference point to ensure the crack tip stress intensity factor K_I=10 MPa·m$^{1/2}$ [9]. Two analysis steps are set. The first one is the loading process, which produces elastic-plastic deformation on the sample; The other is the process of constant load, setting the creep equivalent time to 1000 hours.

3. Results and Discussion

3.1. Effect of cold working on Mises stress around crack tip

The Mises stress distribution around the crack tip under different CW before and after creep is shown in Figure 5 and Figure 6, respectively. Figure 5 shows that Mises stress decreases with increasing of the CW before creep. Figure 6 shows that Mises stress tends to be the same under different CW after creep. Creep has great effect on the Mises stress.

(a) Cold working=0% (b) Cold working=10% (c) Cold working=20%

Figure 5. Comparison of the Mises stress distribution around crack tip before creep (MPa)

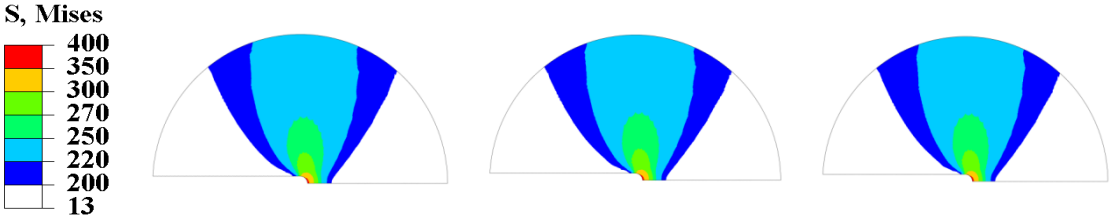

(a) Cold working=0% (b) Cold working=10% (c) Cold working=20%

Figure 6. Comparison of the Mises stress distribution around crack tip after creep (MPa)

3.2. Effect of cold working on PEEQ around crack tip

The PEEQ distribution around the crack tip under different CW before and after creep is shown in Figure 7 and Figure 8, respectively. Figure 7 shows that cold working has little effect on the high PEEQ zone near crack front, but can cause low PEEQ zone decreases with increasing of the CW. Compared Figure 7 with Figure 8, CW has little effect on the PEEQ.

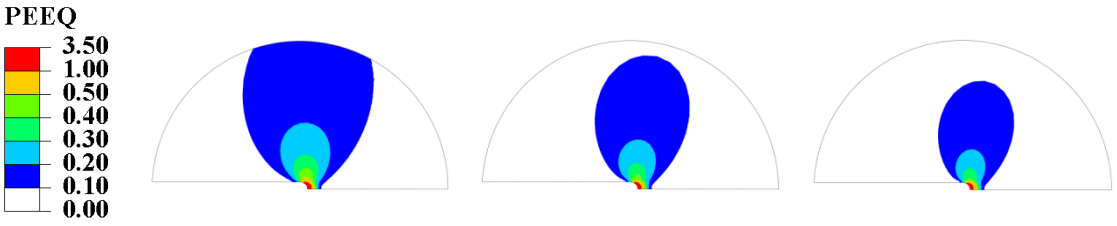

(a) Cold working=0% (b) Cold working=10% (c) Cold working=20%

Figure 7 Comparison of the creep strain distribution around crack tip before creep

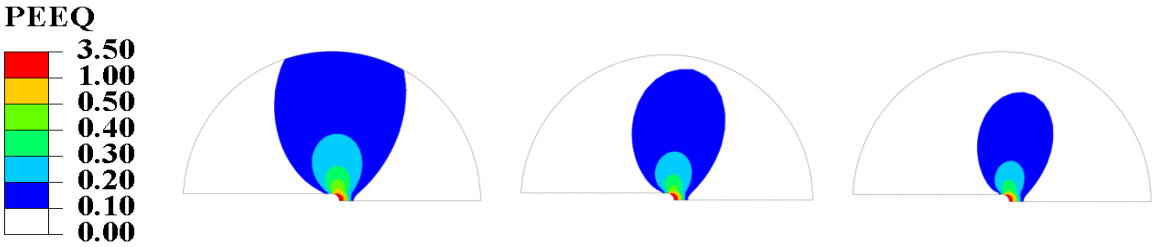

(a) Cold working=0% (b) Cold working=10% (c) Cold working=20%

Figure 8. Comparison of the creep strain distribution around crack tip after creep

3.3. Effect of specimen thickness on SCC crack tip creep strain

The creep strain distribution around the crack tip under different CW is shown in Figure 9. which shows that creep strain increases with the increasing of CW, indicating that the cold working will accelerate stress corrosion cracking to some extent.

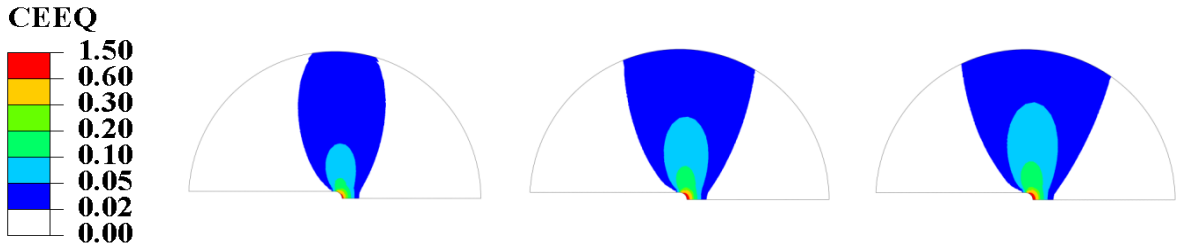

(a) Cold working=0% (b) Cold working=10% (c) Cold working=20%

Figure 9. Comparison of the creep strain distribution around crack tip

4. Conclusions

(1) CW will increase the Mises stress at the crack tip before creep, and the stress around crack tip will release because of creep. As the creep process going on, the effect of CW on the Mises stress around crack front will become weaker;

(2) CW will cause the decrease of the low-plasticity strain region at the crack front, but has little effect on the high plastic strain; CW will also cause the crack tip creep strain increase to a certain extent, indicating that the CW will accelerate stress corrosion cracking to some extent.

Acknowledgements

This work is financially supported by the National Natural Science Foundation of China (Grant Nos. are 11502195 and 2018QDJ009).

References

[1] Andresen P L, Karen G, Lawrence N J. Stress Corrosion Cracking of Sensitized Type 304 Stainless Steel in 288C Water: A Five Laboratory Round Robin[M]. *John Wiley & Sons, Inc*. 2013.

[2] Hou Juan, Peng Qunjia, Shoji Testuo et al. Study of microstructure and stress corrosion cracking behaviour in welding transition zone of Ni-based alloys[J]. *ACTA METALLURGICA SINICA*, 2010, 46(10): 1258-1266.

[3] Zhang L, Chen K, Du D, et al. Characterizing the effect of creep on stress corrosion cracking of cold worked Alloy 690 in supercritical water environment[J]. *Journal of Nuclear Materials*, 2017, (492): 32-40.

[4] Peng Qunjia, Xue He, Hou Juan. Role of water chemistry and microstructure in stress corrosion cracking in the fusion boundary region of an Alloy 182-A533B low alloy steel dissimilar weld joint in high temperature water[J]. *Corrosion Science*, 2011, 53(12): 4309-4317.

[5] Donghai Du, Kai Chen, Hui Lu et al. Effects of chloride and oxygen on stress corrosion cracking of cold worked 316/316L austenitic stainless steel in high temperature water[J]. *Corrosion Science*, 2016, (110): 134-142.

[6] J. Hou, T. Shoji, Z. P. Lu et al. Residual strain measurement and grain boundary characterization in the heat affected zone of a weld joint between Alloy 690TT and Alloy 52[J]. *Journal of Nuclear Materials*, 2010, 397(1): 109-115.

[7] ASTM Standard E399-90. Annual book of ASTM standards[M]. *USA: ASTM International*, 2002.

[8] Quintero H, Mehmanparast A. Prediction of creep crack initiation behaviour in 316H stainless steel using stress dependent creep ductility[J]. *International Journal of Solids & Structures*, 2016, 97–98(10): 101-115.

[9] Xue He, Guo Rui, Chen Zheng, et al. Effect of oxide film thickness on creep at tip of stress corrosion cracking[J]. *China Sciencepaper*, 2016, 22(11): 2619-2622.

[10] Cui Yinghao, Xue He, Zhao Lingyan. Effect of creep property mismatch on mechanical field at crack tip of stress corrosion cracking[J]. *Hot working technology*, 2017, 46(12): 81-85.